ACS APPLIED NANO MATERIALS

www.acsanm.org

Article

Functional Group Effects on the Electrochemical Properties of Carboranethiol Monolayers on Au(111) As Studied by Density Functional Theory: Implications for Organic Electronics

Merve Yortanlı, M. Fatih Danışman, and Ersen Mete*

Cite This: *ACS Appl. Nano Mater.* 2022, 5, 11185−11193

Read Online

ACCESS | Metrics & More | Article Recommendations | Supporting Information

ABSTRACT: Positional isomers of dicarba-closo-dodecaboranethiols with various functional groups (−NO_2, −CHO, −$CONH_2$, −F, −Cl, and −OH) were considered on Au(111) forming (3 × 3) and (5 × 5) structures. Dispersion corrected density functional theory calculations reveal the influence of functional groups on the adsorption characteristics of these carboranethiols depending on the coverage. Functionalized molecules not only possess fascinating chemical and electronic properties but also show stronger chemisorption profiles on gold in relation to the pristine precursors. Molecular dipole moments which can be modified by functional groups were found to be effective in tunability of the work function of deposited surfaces. Results indicate that densely packed adsorption geometries in which functional groups lean toward back of adjacent molecules allowing H-bonding are energetically favorable and enhance stability and ordering of constituents in self-assembled monolayers. Carboranethiols with functional groups are promising to enrich the surface electrochemical properties of resulting surfaces.

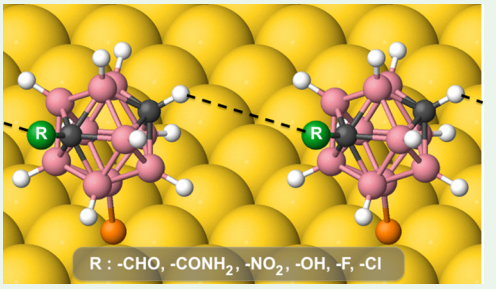

KEYWORDS: *self-assembled monolayer (SAM), carboranethiol, adsorption, functional groups, gold surface*

INTRODUCTION

Self-assembled monolayers of thiols continue to enjoy intense interest and research efforts due to their applications in many different fields ranging from organic electronics to medicine.[1−8] Since the early days of research on alkanethiols, our fundamental understanding of these systems matured immensely and research efforts have shifted to designing new types of thiol molecules for tuning surface properties in a more controlled way appropriate for specific applications.[1,2,7,9] Aromatic thiolate self-assembled monolayers (SAMs) are also used for electrostatic engineering of surfaces and interfaces, including Au(111).[10,11] Carboranethiols (CTs) are boron cluster-based thiols with promising properties due their rigid structure and higher chemical and thermal stability when compared with their organic counterparts.[9,12−25] Defects present in many different thiol SAMs (specially alkanethiols), which limit their use, are minimized in CT SAMs. In addition, due to the unique structure of these clusters, their chemical/electronic properties can be tuned in a very controlled way by varying the position of the sulfur atom and the functional groups on the cluster. Hence, they can be utilized to tune the properties of metal surfaces, which is an essential requirement for all the applications discussed above.

In their pioneering work, Baše et al. studied SAMs of several CTs including 1-HS-1,2-$C_2B_{10}H_{11}$ (*ortho*-carboranethiol) on gold surfaces and reported extraordinary stability toward oxidation and heating.[12] Weiss and co-workers investigated 1-SH-1,7-$C_2B_{10}H_{11}$ (M1) and 9-SH-1,7-$C_2B_{10}H_{11}$ (M9) *meta*-carboranethiol SAMs and were able to tune the work function of gold surfaces by utilizing the different dipole moments of these two isomers. In addition, they found M1 SAMs to have higher affinity to the gold surface due to parallel alignment of the dipole moment of this molecule to the surface,[20] which was later confirmed by computational studies, as well, by others.[22] Work function tunability was also demonstrated by using mixed SAMs of these CTs,[21] in addition to dithiols.[15,21] Both pristine and mixed CT SAMs were shown to have an ordered, densely packed film structure with a hexagonal lattice with a nearest neighbor distance of about 7.2 Å. Though, codeposition (mixed SAMs) of alkanethiols was used in the past for work function tuning purposes, they suffer from increased defect density and changing crystal structure and/or morphology due the flexible nature of the employed molecules, which is not the case for CTs. Building on the promising results of the above mentioned studies, recently interest in this field has shifted to functionalized CT derivatives.[17,19,26] To this end, carboxylic acid-functionalized *meta* (1-COOH-7-SH-1,7-$C_2B_{10}H_{10}$ and 1-COOH-9-SH-1,7-$C_2B_{10}H_{10}$) and *para* (1-

Received: May 28, 2022
Accepted: August 2, 2022
Published: August 12, 2022

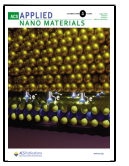

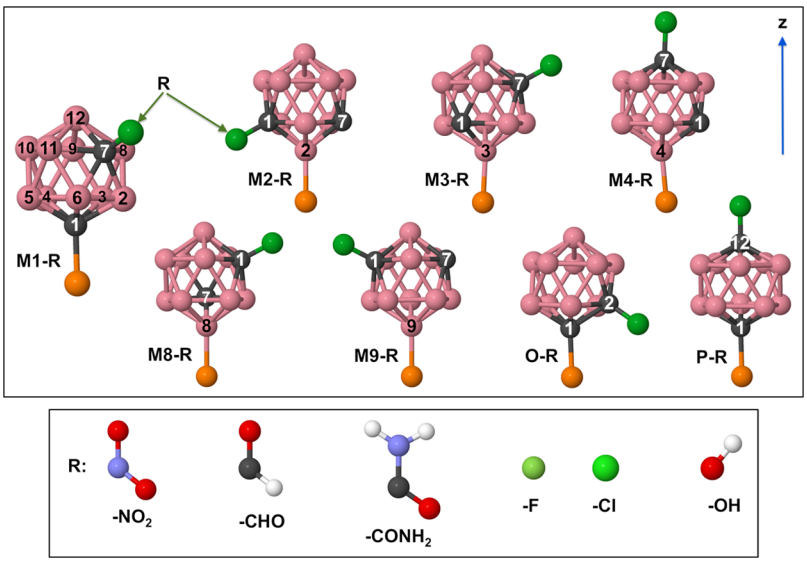

Figure 1. Gas-phase 1−7 *meta*, *ortho*, and *para* CT molecular geometries optimized using the SCAN+rVV10 DFT functional. H atoms are not shown for clear schematic illustration. Colors assigned to indicate different atomic species (pink for boron, black for carbon, orange for sulfur, red for oxygen, white for hydrogen, and blue for nitrogen). Labeling of molecules follows from the attachment position of S to the carborane cage.

COOH-12-SH-1,12-$C_2B_{10}H_{10}$) CTs were investigated by experimental and computational means. Both *para* and *meta* carboxylic acid-functionalized CTs were shown to adapt a densely packed, ordered film structure with a hexagonal unit cell on the gold surface. However, the steric demands imposed by the carboxylic acid functional group in the *meta* isomers increased the nearest neighbor distance to 8.4 Å,[19] whereas for the *para* carboxylic acid-functionalized isomer, this distance was identical to that measured for the unfunctionalized parent molecules (7.2 Å).[17] In addition, the acidities of the carboxyl groups were shown to decrease upon adsorption of these molecules on the gold surface, which was attributed to intermolecular interactions in the SAM.[19]

Motivated by these studies and the agreement between experimental and computational results, we set out to study the effect of different functional groups on the CT SAM properties, with the hope that our findings can guide experimental studies in choosing the appropriate functional group for the desired purpose/application. To this end, we studied $-NO_2$ (strong electron withdrawing), −CHO, $-CONH_2$ (moderate electron withdrawing), −F, −Cl (weak electron withdrawing), and −OH (strong electron donating) functionalized *ortho*, *meta*, and *para* CTs on gold surfaces by using dispersion corrected density functional theory (vdW-DFT).

COMPUTATIONAL DETAILS

As a d-band transition metal, gold forms metallic surfaces where electronic correlations become important. To study the molecular adsorption morphologies, the methodology must be sensitive not only to the flatness of the potential energy surface of defect-free Au(111) but also to the degree of molecule−metal and intermolecular interactions. Previously, we showed that DFT-based calculations can successfully predict energetics and structures of CT adsorption on Au(111) consistent with experiments.[26] The projector augmented wave method was used as implemented in the Vienna ab initio simulation package.[27−29] Single particle Kohn−Sham orbitals were expanded in the plane wave basis up to a kinetic energy cutoff of 400 eV. To enhance computational description of electronic correlations and to include dispersive corrections, SCAN +rVV10[30] was used as the exchange and correlation (XC) functional. SCAN+rVV10 combines meta-GGA nonempirical and semilocal SCAN[31] XC formalism with a nonlocal rVV10 (revised Vydrov−van Voorhis)[32] correlation functional. This method gave the best estimate for the lattice parameter of bulk gold among standard DFT functionals, some of which were supplemented with various flavors of (van der Waals) vdW corrections.[33] Moreover, the interaction between graphene (and also the benzene molecule) and M(111) (M = Ni, Cu, Au) is better described with the SCAN+rVV10 functional among benchmarked vdW corrected DFT functionals in regard to experimental data.[30,33−35]

Labeling of CT molecules based on the positional isomerization of two carbon atoms on the borane cage was discussed previously[26] and is illustrated in Figure 1. The carborane cages are different for the isomers in regard to the positions of the two carbon atoms. We considered attachment of the functional groups at one of the carbon sites, if possible at the upper part of the cage, where they can be exposed to the environment from the SAM. The same idea was previously used in the synthesis of COOH-functionalized M1 and M9.[17,19] It is important to point out that a detailed quantum chemistry study of the CT isomers is still needed where the stabilization energies from each functional group in each position would be taken into account. Explicit and accurate prediction of the stabilization energies of functionalized CT isomers might require a quantum chemistry code, which employs Gaussian basis sets and probably a higher level of theory applicable to molecular structures. Technically, our plane wave basis approach for the extended systems suits better for the slab calculations assuming periodic boundary conditions (PBC). To represent the metal surfaces, slab models were constructed by replication of the bulk unit cell of gold. The supercells contain the Au(111) slab with four atomic layers, molecular CT adsorbates, and a vacuum region with a thickness of at least 12 Å along the surface normal. The study of isolated and dense molecular chemisorption cases requires

https://doi.org/10.1021/acsanm.2c02339
ACS Appl. Nano Mater. 2022, 5, 11185−11193

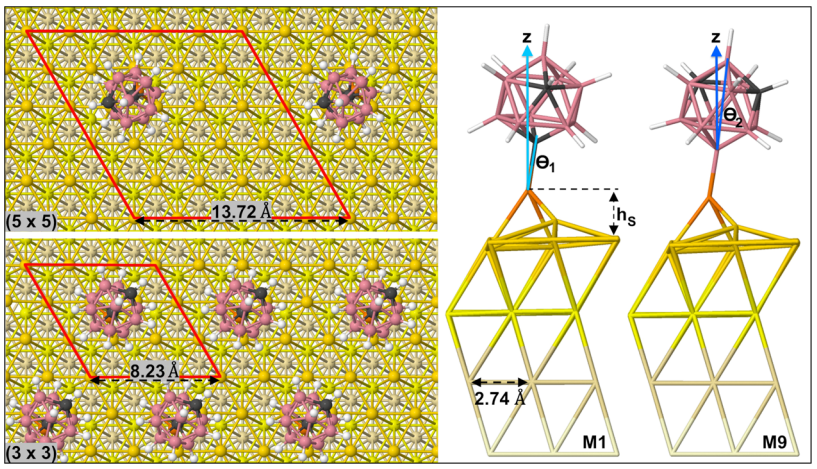

Figure 2. On the left: Top views of CT adsorption geometries on Au(111) with (3 × 3) and (5 × 5) structures. On the right: The side views of chemisorption of M1 and M9 isomers on Au(111). The schematics show the tilting angles θ_1 and θ_2 as well as the height of the S atom from the surface plane, h_S. Atomic layers in the gold slab were depicted with different shades from orange to pale yellow.

(5 × 5) and (3 × 3) cells of Au(111) to be built as shown in Figure 2. The nearest neighbor distance between the CT molecules on the surface is 13.72 Å on the (5 × 5) structure and is 8.23 Å on the (3 × 3) structure. Three probable adsorption sites were considered at the bridge, the hollow, and the top positions on the hexagonal coordination of the surface gold atoms (as shown in Figure S2 of the Supporting Information). Surface morphologies such as domain boundaries observed on the thiolate SAMs on gold cannot be realistically simulated basically because of the size of the Hamiltonian matrix to be diagonalized, which restricts the surface area of a computational slab model to a few nm^2. Therefore, the number of atoms in a supercell is typically less than a thousand atoms.

The first Brillouin zones of (3 × 3) and (5 × 5) supercells were sampled using Γ-centered 8 × 8 × 1 and 5 × 5 × 1 uniform *k*-point meshes, respectively. A smearing parameter of 0.05 was included in the calculations using the Methfessel–Paxton scheme. The geometric optimizations of each computational model were carried out by requiring the Hellmann–Feynman forces in three spatial directions on each atom to be less than 10^{-2} eV/Å. The dipole corrections were also considered throughout the calculations.

The ground-state energy of a system of electrons and nuclei is estimated by means of variational minimization as being one of the pillars of the DFT method. Once coupled with the supercell approach, for periodic structures, the total cell energy can be regarded as the best possible estimate (depending on the XC scheme) to the true ground state of the system, which is modeled in a cell assuming PBC. Then, experimentally accessible energies reflecting the main characteristics of surface structures, such as work functions, surface energies, adsorption energies, etc., can be predicted by performing DFT calculations using appropriate supercell models. In this manner, the dissociative chemisorption energies of pristine and functionalized CTs, which were examined at different coating densities on the Au(111) surface, were calculated as follows:

$$E_c = \frac{E_{CT+Au(111)} - E_{Au(111)} - n(E_{CT} - E_H)}{n}$$

where $E_{CT + Au(111)}$ is the total cell energy obtained with a number of CT molecules (n) on the Au(111) surface. $E_{Au(111)}$ and E_{CT} are the total energies of the clean Au(111) surface cell and the gas-phase energy single CT molecule, respectively. E_H is the energy of the hydrogen atom derived from, $E_H = E_{H_2}/2$, molecular hydrogen.

RESULTS AND DISCUSSION

A total of 48 different CT derivatives were considered by means of 8 positional isomers and 6 functional groups (R: $-NO_2$, −CHO, $CONH_2$, −F, −Cl, and −OH), which were attached at the carbon sites to be exposed to the environment as indicated in Figure 1. DFT geometry optimizations were carried out as step-by-step iterations where all atomic coordinates were updated based on the minimization of forces and the total energy, as a search for the global minimum of the potential energy surface. From the initial configurations to the final relaxed structures, these iterations implicitly change the orientation of the functional groups while optimizing the CT-R geometry. The energy as a function of positional isomerization shows similar characteristics for the CT-R molecules in each of the R-groups considered here, as seen in Figure 3. The relative energies of CT derivatives show a strong dependence on the positional isomerization rather than on the functional group. Based on the thiol attachment position on the cage, all the C-substituted carborane isomers (O, M1, and P) show generally lower stability compared with the B-substituted ones. In the gas phase, M2, M3, M4, M8, and M9 variants always have lower energies relative to the remaining isomers. DFT calculations show that M9 is almost 1 eV lower in energy than M1. Moreover, this energy difference is preserved in the presence of different functional groups. The CT derivatives are anchored to the gold surface through their thiol terminals and that allows the self-assembly of these polar molecules on the surface. Pristine M1 and M9 isomers were particularly considered by many experimental studies due to their mutually perpendicular dipole moments, which influence the morphology and electronic properties of SAMs.[9,15,20] M1 has a parallel dipole moment on the surface, while M9 has a dipole moment perpendicular to the surface plane. The molecular dipole moment is determined by positional isomerization of carbon atoms on the rhombohedral borane cage and also by additional functional groups (Table S2, Supporting Information).

https://doi.org/10.1021/acsanm.2c02339
ACS Appl. Nano Mater. 2022, 5, 11185−11193

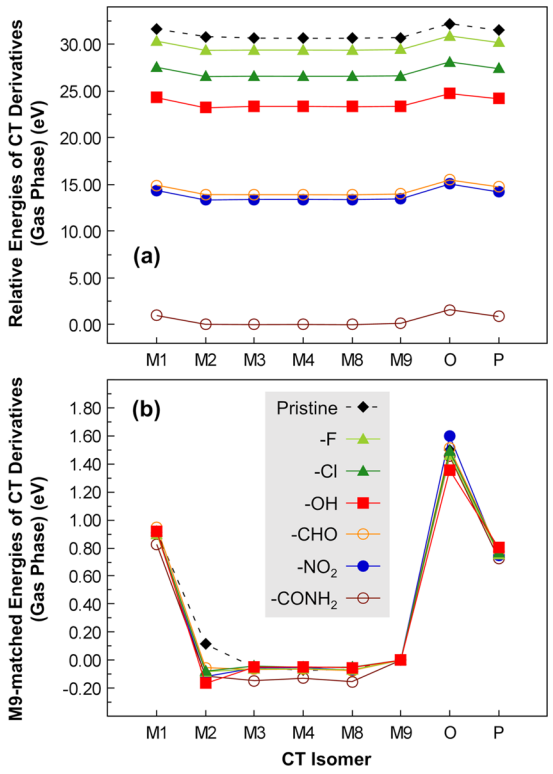

Figure 3. Gas-phase energies of the functionalized CTs with respect to positional isomerization, relative to (by subtraction) (a) that of CT-$CONH_2$ and (b) their M9 isomers.

The dissociative adsorption of each of the CT derivatives was considered with (3 × 3) and (5 × 5) structures on Au(111). The former corresponds to the densely packed coverage, while the latter can be considered as isolated molecules on the surface. The optimized geometries of the complete set of CT derivatives are depicted in Figure S3 through Figure S98 (Supplementary Information). The strongest binding cases of CT-Rs on the metal surface are shown in Figure 4 separately for each of the functional groups.

The calculations performed using the SCAN+rVV10 functional predict accurate interlayer properties in comparison with the experimental data.[36] The DFT predictions indicate that pristine CT isomers get anchored by their thiol terminals on the Au(111) surface close to the bridge site where the sulfur atom tends toward the hollow site and pulls up the surface gold atom just across the bridge position (in Figures S3−S10 and S59−S73 of the Supporting Information). The height of the pulled-up gold atom from the surface plane is between 0.52 and 0.80 Å on the (5 × 5) structure and gets larger for the (3 × 3) cases where the tilting angles are relatively small (in Tables S3 and S10 of the Supporting Information). This finding was also reported in previous theoretical studies.[26] In addition, the phenomenon that a gold atom being pulled up by the thiol terminal as a result of Au−S bond formation mimics the adatom model used to explain the experimental observations regarding self-assembly of thiolates on Au(111).[37−40]

The adsorption pattern in the form of perturbed coordinates of the three surface Au atoms in interaction with the pristine CTs as described here is also followed in the Cl- and F-functionalized CT cases (Figures S35−S50, S87−S93, and Tables S7, S8, S14, and S15 of the Supporting Information). For the remaining cases, depending on the functional group, more than one Au atom can be below or above the surface plane. In particular, M2-$CONH_2$ on the (5 × 5) structure pushes down all three nearest neighbor Au atoms at the adsorption site below the surface plane.

CT-R Chemisorption on Au(111)-(5 × 5). The energy profiles of molecules in the gas phase in Figure 3a and of isolated molecules on Au(111) in Figure 5a reflect similarities with respect to positional isomerization. The total cell energy refers to the ground-state energy of the corresponding model structure. From a theoretical point of view, isomers have equal numbers of atoms and are composed of the same species. Spatial atomic configurations of otherwise equivalent structures end up with different total cell energies. This could be seen as relative stability of isomers with respect to each other. For instance, the total cell energies of *ortho* CTs were found to be considerably higher with respect to those of other isomers. In

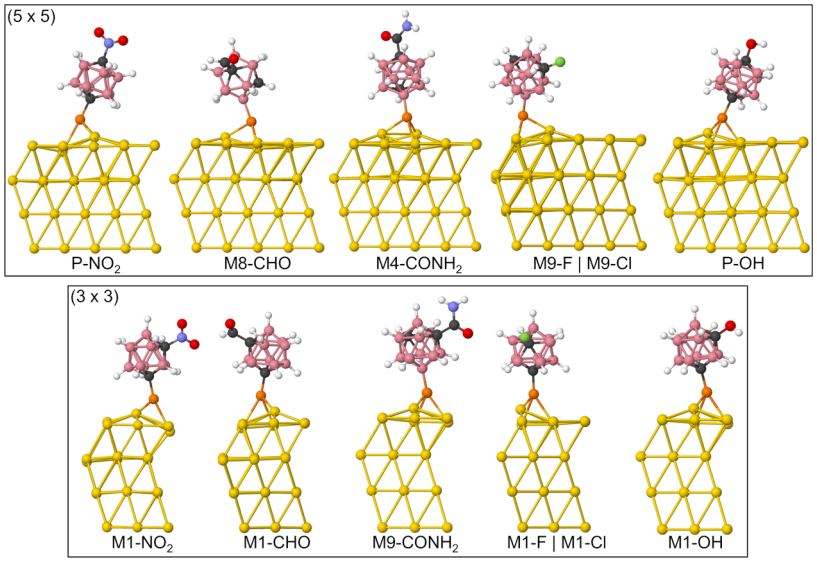

Figure 4. For each functional group case, the minimum energy geometries of CT-Rs (R = $-NO_2$, −CHO, $-CONH_2$, −F, −Cl, −OH) on Au(111) slabs with (5 × 5) and (3 × 3) structures, which were optimized using the SCAN+rVV10 DFT functional, are depicted.

https://doi.org/10.1021/acsanm.2c02339
ACS Appl. Nano Mater. 2022, 5, 11185−11193

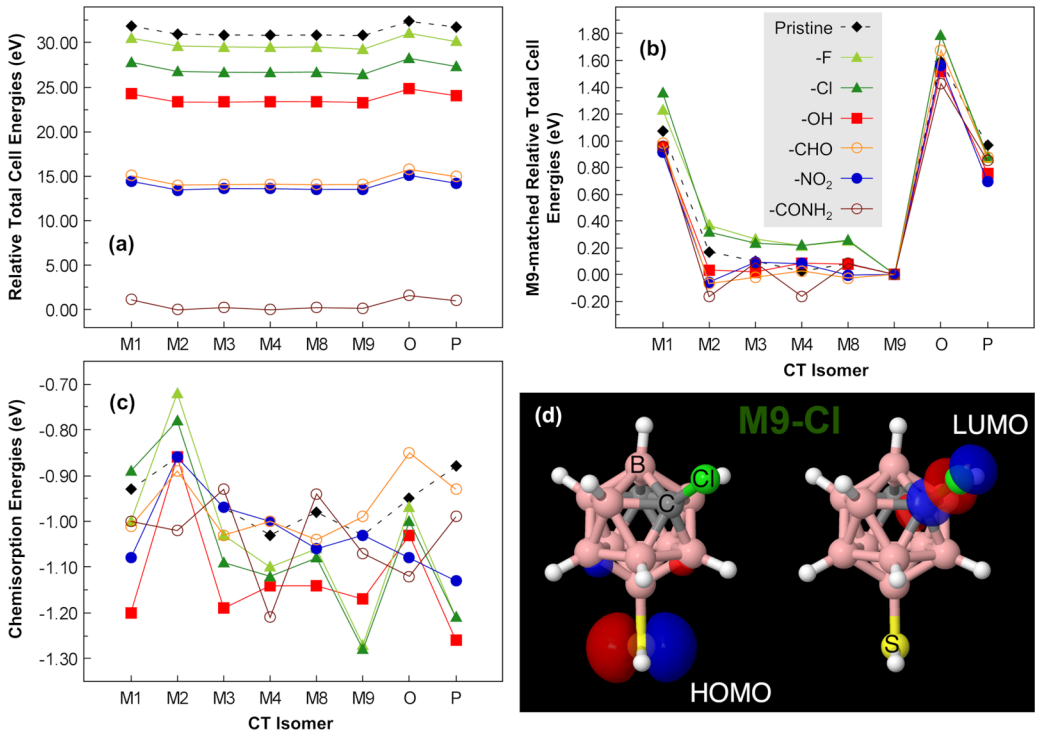

Figure 5. Computational cell energies of the pristine and functionalized CT isomer/Au(111)-(5 × 5) systems, relative to (a) that of M4-$CONH_2$, and (b) their M9 isomers. (c) Dissociative chemisorption energies of CT-Rs on the (5 × 5) structure calculated using the SCAN+rVV10 DFT functional. (d) Spatial visualization of HOMO and LUMO of M9-Cl (E_c = −1.28 eV).

addition, a comparison of the chemisorption energies in Figure 5c reveals that *ortho* and M2 isomers generally end up with the weakest binding to the gold surface. The main reason behind this result is the attachment position of the functional groups being at the lower part of the carborane cage closer to the thiol terminal. In this configuration, the functional groups distort the adsorption geometry and make it difficult to form a strong binding with the surface. One exception of this trend is seen in the case of M2-$CONH_2$ and O-$CONH_2$ due to relatively long $CONH_2$ groups being almost parallel to the Au surface at an interaction height (i.e., O−Au distance is 3.17 Å). When a ligand lies over and weakly interacts with metal surface, this contribution increases the chemisorption energy in magnitude (Figures S28 and S33, Supporting Information).

The chemisorption energies change in a range of 0.56 eV between the weakest (M2-F, E_c = −0.72 eV) and the strongest (M9-Cl, E_c = −1.28 eV) chemisorption cases among the derivatives considered on Au(111)-(5 × 5). When M2 and *ortho* isomers are excluded from Figure 5c, the fluctuation of the chemisorption energies fits within a narrower interval. Then, the results are in close vicinity of typical S−Au bond formation energy. In fact, the HOMO of each of the CT-Rs is largely contributed by 3p electrons of S atoms, which act as the anchoring agent at the thiol terminal. Other factors that influence the adsorption characteristics are the positional isomerization and additional functional groups, which significantly influence the spatial charge distribution on the molecules modifying the overall dipole moment. To elaborate the role of the molecular dipole moment in the adsorption energies, the calculations have been performed on CT-Rs in the gas phase where the *z* direction of the computational cell is aligned with the major axis of the molecules. The results (in Table S2 of the Supporting Information) are given in the convention that the dipole moment points from relatively positive to negative charge. The calculated data for the pristine CTs were given elsewhere.[26] An isolated adsorbate with a dipole moment in the direction away from the surface is favorable because the thiol terminal being the relatively positively charged part of the CT has a strong electron affinity and forms an S−Au bond as a result of electron transfer from the metal to the S atom. One can note that a dipole moment with a negative z-component generally indicates a weaker binding for the isolated and small thiolates on the gold surface. This trend is consistent for CT derivative cases with rather small functional groups, which do not significantly change the dipole moment of the parent molecule. For instance, the chemisorption of the *ortho* and M2 variants in the cases of −F, Cl, −OH, and −CHO cases is significantly weaker. In addition, NO_2-functionalized M2 and M9 isomers follow the same trend. However, a generalization based on the overall dipole moment is not possible for relatively large (electron rich) and polar functional groups such as $CONH_2$, which extends away from the carborane cage. Upon attachment to the CT parent, it significantly influences the overall dipole moment. On the (5 × 5) surface structure, M9 and *para* isomers give strong chemisorption with −Cl, −F, and −OH. The calculations reveal that these three functional groups are effective in enhancing the binding of isolated CTs on the gold surface. In particular, the electron-donating hydroxyl group significantly increases the magnitude of the adsorption energy of CTs with the exception of the M2 isomer, which always ends up with low binding as stated earlier. Similarly, weak electron-withdrawing halogen groups increase the binding strength of CTs with the exception of the M1-Cl, M2-Cl, and M2-F isomers for which the adsorption is even weaker relative to that of the pristine cases.

https://doi.org/10.1021/acsanm.2c02339
ACS Appl. Nano Mater. 2022, 5, 11185−11193

CT-R SAMs on Au(111)-(3 × 3). In a recent experiment, COOH-functionalized M1 and M9 SAMs were observed to form a (3 × 3) structure on Au(111).[19] Following this experimental observation, in this study, we report the effect of the other possible functional groups (−NO_2, −CHO, $CONH_2$, −F, −Cl, and −OH) on the adsorption characteristics of M1 and M9 isomers on the gold surface at full monolayer coverage. The stark influence of positional isomerization of CT molecules on the total computational cell energies is once again shown for the (3 × 3) structures in Figure 6a similar to

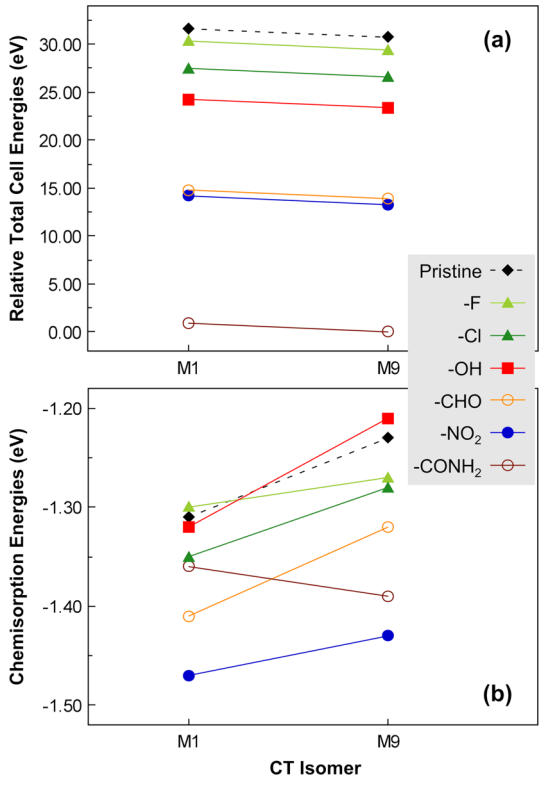

Figure 6. vdW-DFT results of (a) relative total cell energies referenced with respect to the case of the M9-$CONH_2$ group, and (b) chemisorption energies of the functionalized M1 and M9 CT isomers on Au(111)-(3 × 3).

the (5 × 5) cases in Figure 5a and the gas phase cases in Figure 3a. The slopes in Figure 6a indicating energy differences between M1 and M9 derivatives are almost the same for all the functional groups. Adsorption energy is one of the key factors affecting the stability of the adlayer on the metal. The calculated chemisorption energies of CT derivatives at one full monolayer coverage (in Figure 6b and Tables S10−S16 of the Supporting Information) significantly increase in magnitude relative to those on the (5 × 5) cell structures (in Figure 5c and Tables S3−S9 of the Supporting Information). On the average, dense packing of pristine CTs at the (3 × 3) structure corresponds to an increase of approximately 32.5% in the molecular chemisorption energy relative to the adsorption on the (5 × 5) surface cell. Moreover, the DFT calculations showed that the functionalized CT isomers get chemisorbed on the surface even stronger than their pristine counterparts. A similar trend due to intermolecular interactions was reported previously for COOH-functionalized M1 and M9 isomers on Au(111)-(3 × 3).[19] Pristine CTs were previously considered as a protective coating on metals.[14] The significant increase brought by the functional groups in the adsorption energies at 1 ML has implications for durability and corrosion resistance of functionalized CT SAMs on metal surfaces. Intermolecular distances become 60% shorter on the (3 × 3) cell with respect to those on the (5 × 5) cell. Dense packing results in significantly larger intermolecular interactions in the SAMs. The DFT calculations including long-range dispersive forces showed that intermolecular interactions have an important impact on stabilization and ordering of molecules within SAM structures. Experimental studies reported hydrogen bonding networks within amide-functionalized thiolates and revealed that amide-based H-bonds extend across molecular domain boundaries.[41−43] The dispersive corrected DFT results can be partly interpreted as intermolecular interactions can extend over long ranges within densely packed CT-R SAMs.

As discussed earlier, the M1 isomer is energetically less preferable among the other isomers on the (5 × 5) cell for most of the cases where the dipole moment is nominally parallel to the surface. For the pristine cases, a well-organized dense packing at the (3 × 3) structure favors the M1 isomer over the M9 isomer.[20,22,26] At full 1 ML coverage, a dipole parallel to the gold surface is more preferable due to dipole−dipole interactions. The calculated chemisorption energies on the (3 × 3) structure as given in Figure 6 reveal that the M1 isomer is still more favorable than the M9 isomer for each functional group except the $CONH_2$ case. The functionalized CT-Rs have different sizes, geometries, and numbers of total electrons. Therefore, the orientation of the dipole moment changes with respect to their pristine counterparts. A codeposition of different derivatives (by isomerization or by functional groups) with opposing dipole moments influences the morphologies of the resulting mixed SAMs as observed in experiments for the pristine isomers.[23] In addition to these considerations, dense packing of CT-Rs at the (3 × 3) structure leads to H-bonding as a result of tilting of the parent molecule and leaning of functional groups toward the adjacent carborane cage. Spatially, the H-bonding is effective at a shorter distance while dipole−dipole interactions acting at a longer intermolecular separation. Therefore, H-bonding between the adjacent molecules in the cases of M1-NO_2, M9-NO_2, M1-CHO, and M9-$CONH_2$ leads to the strongest chemisorption among the other derivatives (Figures 6 and S76, S78, S80, and S86 of the Supporting Information). Their optimized geometries, the dipole moments, and the H-bonds are depicted in Figure 7. The dipole moment alignment of CT molecules is especially important at interfaces in interaction with polar molecular environments. For instance, application of external fields or deposition of molecular adlayers with different electronic properties can be controlled to modify anchoring, tilting, or even rotation of molecules in the CT SAMs.[18,25] The atomistic simulations bring a lot of details to the table. For instance, the molecules have tilting angles, S−Au bonds tilted, and also the cage gets another tilting angle on the gold surface. Moreover, adsorption causes local perturbation on the interacting Au atoms. Considering molecular rotations on the surfaces, top of these tilt angles and local surface distortions give rise to many possibilities. Even though we did not attempt to profile energy barriers of rotation of CT-Rs around S−Au bonds, our results on the (3 × 3) cell indicate that such a rotation would be hindered for the NO_2-, CHO-, and $CONH_2$-functionalized M1 and M9 cases due to in-plane H-bonding networks. In agreement with recent experimental and theoretical studies,[19,26] the hydrogen bonding has an

https://doi.org/10.1021/acsanm.2c02339
ACS Appl. Nano Mater. 2022, 5, 11185−11193

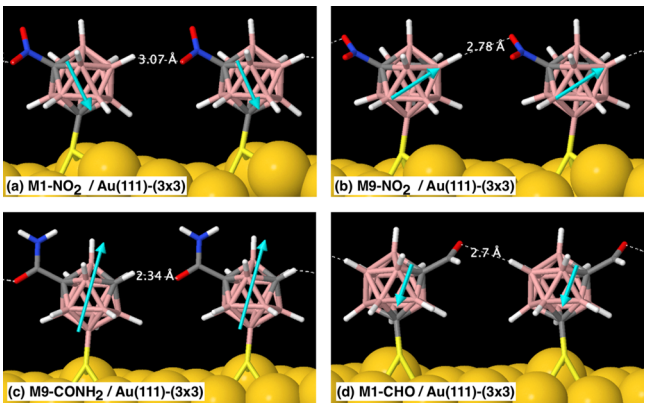

Figure 7. Optimized geometries of high chemisorption conformations of (a) M1-NO_2, (b) M9-NO_2, (c) M9-$CONH_2$, and (d) M1-CHO SAM structures on Au(111) showing a (3 × 3) order, which is driven by H-bonding between O and H sites of the adjacent molecules. The dipole moments are illustrated by the arrows.

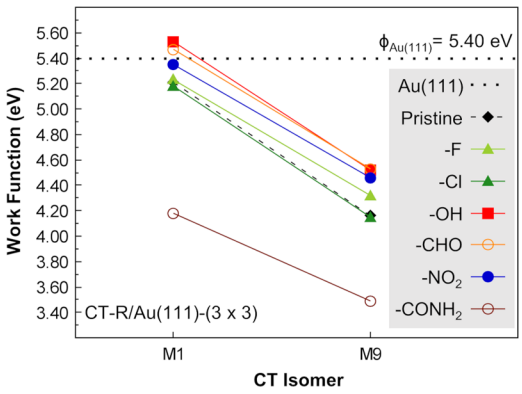

Figure 8. Calculated work functions of the Au(111) surface coated with M1 and M9 derivatives (functionalized by −F, −Cl, −OH, −CHO, $-NO_2$, and $-CONH_2$ groups) having (3 × 3) periodicity. The work function of the bare Au(111) surface is indicated with a horizontal dotted line at 5.40 eV.

enhancing effect on ordering of functionalized CTs in SAMs. The functionalized CTs usually end up with larger chemisorption energies, in magnitude, relative to the pristine cases with the exception of M9-OH and M1-F. Moreover, at 1 ML coverage, CTs with a halogen or a hydroxyl group show characteristics similar to their pristine cases. Consequently, functional group attachment not only enhances the adsorption strength of CT molecules on Au(111) but also plays an important role in improving the stability of SAMs. In addition, the lowest energy conformations as shown in Figure 7 lead to a molecular organization where the functional groups are exposed to the environment.

Experimental studies showed that adsorption of M1 and M9 isomers on the gold surface shifts the work function.[17,20] In addition to positioning of the carbon atoms on the carborane cage, attachment of functional groups to one of these carbon atoms also is expected to play an important role in modifying the surface electronic properties. In this regard, the vdW-corrected DFT calculations were performed using the SCAN +rVV10 functional. The results (in Table 1) reveal that the carborane cage (e.g., as in M1 or M9) has a strong effect on the electronic properties of the SAMs consistent with experiments.[17,20] Moreover, significant modification of the work function is possible through functionalization of CTs by attaching different electron acceptor/donor groups at the carbon sites on the carborane cage as given in Table 1 and as schematically shown in Figure 8.

Table 1. Calculated Work Functions, Φ, of the CT-R-Coated Au(111) Substrate with (3 × 3) Structure

	Φ (eV)						
	CT-R/Au(111)-(3 × 3)						
CT isomer	CT	CT-F	CT-Cl	CT-CHO	CT-$CONH_2$	CT-NO_2	CT-OH
M1	5.21	5.23	5.18	5.47	4.18	5.35	5.53
M9	4.16	4.32	4.15	4.53	3.49	4.46	4.52

The effect of the M1 isomer on the work function is smaller than that of the M9 isomer, which is consistent with previous observations.[20] The M9 isomer significantly decreases the work function of the gold substrate. This effect is attributed to the orientation of the dipole moment being nominally perpendicular to the surface. A similar trend on Pt was recently reported by Ano et al.[44] who used M9 SAMs to decrease the Schottky barrier at the Pt/TiO_2 interface. Their work function measurements are also in line with our findings on Au. M9-$CONH_2$ is a good example resulting in a work function of 3.49 eV with its substantial dipole moment of 6.69 D, as illustrated in Figure 7c. For all the functional groups, the decrease in the work function from the M1 to M9 isomer shows the same trend as indicated in Figure 8. While most of the CT derivatives decrease the work function, M1-CHO and M1-OH groups slightly increase it relative to the clean gold surface. The drop of the work function with the $CONH_2$-functionalized CT coating is significantly larger from the rest of the ligands. As a result, tunability of the work function of the SAMs functionalized by these groups in a wide range between 5.57 and 3.49 eV paves the way for the development of various applications.

CONCLUSIONS

The vdW-DFT calculations reveal that the functional groups enhance the binding of the CT isomers on the gold surface in relation to pristine cases. In particular, isolated M9 and *para* isomers functionalized by the halogen and hydroxyl groups are chemisorbed significantly stronger on the (5 × 5) structure. A net dipole moment pointing away from the surface is always favorable but is not the only factor for the chemisorption characteristics of a single isolated CT isomer on Au(111). In the cases of pristine, Cl-, and F-functionalized CTs, one of the surface gold atoms is pulled up by the thiol end, which mimics the adatom chemisorption model. Adsorption of CTs with relatively larger functional groups causes local perturbations on Au(111) where more than one surface Au atom can be below or above the surface plane. The favorable functional group, among different alternatives considered in this work, changes to the nitro group at one full monolayer coverage based on the chemisorption energy profiles. The nitro-functionalized CTs are followed by M9-$CONH_2$ and M1-CHO, which also exhibit strong chemisorption. These SAM structures are promising for applications such as protection of metal surfaces from corrosion and modification of electronic potential barriers at metal/oxide interfaces. The coverage dependence of this drastic change on the adsorption energies is due to intermolecular interactions. At 1 ML on the (3 × 3) structure, in addition to dipole−dipole interactions within the SAM, H-

https://doi.org/10.1021/acsanm.2c02339
ACS Appl. Nano Mater. 2022, 5, 11185−11193

bonding becomes effective at a shorter distance in the cases where the functional groups lean toward the carborane cage of the neighboring CT-R. Consequently, the chemisorption is significantly stronger when H-bonds are possible, which helps increasing the order and stability of SAMs. In this sense, the positional isomerization together with functional groups is promising for controllability of long-range ordering and stability of SAMs. Moreover, the functional groups offer tunability of the work function over a wide range of 2.08 eV, which is desirable for promoting the usability of the SAM structures. The functional groups exposed to the environment on the SAM structures pave the way to design various applications.

■ ASSOCIATED CONTENT

Supporting Information

The Supporting Information is available free of charge at https://pubs.acs.org/doi/10.1021/acsanm.2c02339.

Molecular structures and DFT-calculated properties of the positional carborane isomers and functional groups, Au(111) slab models, DFT-optimized chemisorption geometries of pristine and functionalized carboranethiol isomers on Au(111)-(5 × 5) and Au(111)-(3 × 3), calculated energies, and structural parameters (PDF)

DFT-optimized atomic coordinates of all the cases in the xyz file format (ZIP)

■ AUTHOR INFORMATION

Corresponding Author

Ersen Mete − *Department of Physics, Balıkesir University, Balıkesir 10145, Turkey;* orcid.org/0000-0002-0916-5616; Email: emete@balikesir.edu.tr

Authors

Merve Yortanlı − *Department of Physics, Balıkesir University, Balıkesir 10145, Turkey;* orcid.org/0000-0002-1956-1196

M. Fatih Danışman − *Department of Chemistry, Middle East Technical University, Ankara 06800, Turkey;* orcid.org/0000-0002-7252-3113

Complete contact information is available at: https://pubs.acs.org/10.1021/acsanm.2c02339

Author Contributions

All authors gave equal contribution to the writing and approval to the final version of the manuscript.

Notes

The authors declare no competing financial interest.

■ ACKNOWLEDGMENTS

E.M. and M.Y. gratefully acknowledge financial support from TUBITAK (The Scientific and Technological Research Council of Turkey) under Grant No. 116F174. The calculations reported in this paper were performed at TUBITAK ULAKBIM, High Performance and Grid Computing Center (TRUBA resources).

■ REFERENCES

(1) Love, J. C.; Estroff, L. A.; Kriebel, J. K.; Nuzzo, R. G.; Whitesides, G. M. Self-Assembled Monolayers of Thiolates on Metals as a Form of Nanotechnology. *Chem. Rev.* **2005**, *105*, 1103−1170.

(2) Schreiber, F. Structure and Growth of Self-Assembling Monolayers. *Prog. Surf. Sci.* **2000**, *65*, 151−257.

(3) Singh, M.; Kaur, N.; Comini, E. The Role of Self-Assembled Monolayers in Electronic Devices. *J. Mater. Chem. C* **2020**, *8*, 3938−3955.

(4) Chen, H.; Zhang, W.; Li, M.; He, G.; Guo, X. Interface Engineering in Organic Field-Effect Transistors: Principles, Applications, and Perspectives. *Chem. Rev.* **2020**, *120*, 2879−2949.

(5) Matharu, Z.; Bandodkar, A. J.; Gupta, V.; Malhotra, B. D. Fundamentals and Application of Ordered Molecular Assemblies to Affinity Biosensing. *Chem. Soc. Rev.* **2012**, *41*, 1363−1402.

(6) Vericat, C.; Vela, M. E.; Benitez, G.; Carro, P.; Salvarezza, R. C. Self-Assembled Monolayers of Thiols and Dithiols on Gold: New Challenges for a Well-Known System. *Chem. Soc. Rev.* **2010**, *39*, 1805.

(7) Vericat, C.; Vela, M. E.; Corthey, G.; Pensa, E.; Cortés, E.; Fonticelli, M. H.; Ibañez, F.; Benitez, G. E.; Carro, P.; Salvarezza, R. C. Self-Assembled Monolayers of Thiolates on Metals: A Review Article on Sulfur-Metal Chemistry and Surface Structures. *RSC Adv.* **2014**, *4*, 27730−27754.

(8) Chaki, N. K.; Vijayamohanan, K. Self-Assembled Monolayers as a Tunable Platform for Biosensor Applications. *Biosens. Bioelectron.* **2002**, *17*, 1−12.

(9) Hohman, J. N.; Claridge, S. A.; Kim, M.; Weiss, P. S. Cage Molecules for Self-Assembly. *Mater. Sci. Eng., R* **2010**, *70*, 188−208.

(10) Asyuda, A.; Wiesner, A.; Wan, X.; Terfort, A.; Zharnikov, M. Charge Transport Properties of Single-Component and Binary Aromatic Self-Assembled Monolayers with Methyl and Trifluoromethyl Tail Groups. *J. Phys. Chem. C* **2020**, *124*, 24837−24848.

(11) Asyuda, A.; Wan, X.; Zharnikov, M. Binary Aromatic Self-Assembled Monolayers: Electrostatic Properties and Charge Tunneling Rates across the Molecular Framework. *Phys. Chem. Chem. Phys.* **2020**, *22*, 10957−10967.

(12) Baše, T.; Bastl, Z.; Plzák, Z.; Grygar, T.; Plešek, J.; Carr, M. J.; Malina, V.; Šubrt, J.; Boháček, J.; Večerníková, E.; Kříž, O. Carboranethiol-Modified Gold Surfaces. A Study and Comparison of Modified Cluster and Flat Surfaces. *Langmuir* **2005**, *21*, 7776−7785.

(13) Baše, T.; Bastl, Z.; Šlouf, M.; Klementová, M.; Šubrt, J.; Vetushka, A.; Ledinský, M.; Fejfar, A.; Macháček, J.; Carr, M. J.; Londesborough, M. G. S. Gold Micrometer Crystals Modified with Carboranethiol Derivatives. *J. Phys. Chem. C* **2008**, *112*, 14446−14455.

(14) Baše, T.; Bastl, Z.; Havránek, V.; Lang, K.; Bould, J.; Londesborough, M. G. S.; Macháček, J.; Plešek, J. Carborane−Thiol−Silver Interactions. A Comparative Study of the Molecular Protection of Silver Surfaces. *Surf. Coat. Technol.* **2010**, *204*, 2639−2646.

(15) Lübben, J. F.; Baše, T.; Rupper, P.; Künniger, T.; Macháček, J.; Guimond, S. Tuning the Surface Potential of Ag Surfaces by Chemisorption of Oppositely-Oriented Thiolated Carborane Dipoles. *J. Colloid Interface Sci.* **2011**, *354*, 168−174.

(16) Baše, T.; Bastl, Z.; Havránek, V.; Macháček, J.; Langecker, J.; Malina, V. Carboranedithiols: Building Blocks for Self-Assembled Monolayers on Copper Surfaces. *Langmuir* **2012**, *28*, 12518−12526.

(17) Thomas, J. C.; Boldog, I.; Auluck, H. S.; Bereciartua, P. J.; Dušek, M.; Macháček, J.; Bastl, Z.; Weiss, P. S.; Baše, T. Self-Assembled *p* -Carborane Analogue of *p* -Mercaptobenzoic Acid on Au{111}. *Chem. Mater.* **2015**, *27*, 5425−5435.

(18) Schwartz, J. J.; Mendoza, A. M.; Wattanatorn, N.; Zhao, Y.; Nguyen, V. T.; Spokoyny, A. M.; Mirkin, C. A.; Baše, T.; Weiss, P. S. Surface Dipole Control of Liquid Crystal Alignment. *J. Am. Chem. Soc.* **2016**, *138*, 5957−5967.

(19) Goronzy, D. P.; Staněk, J.; Avery, E.; Guo, H.; Bastl, Z.; Dušek, M.; Gallup, N. M.; Gün, S.; Kučeráková, M.; Levandowski, B. J.; Macháček, J.; Šícha, V.; Thomas, J. C.; Yavuz, A.; Houk, K. N.; Danışman, M. F.; Mete, E.; Alexandrova, A. N.; Baše, T.; Weiss, P. S. Influence of Terminal Carboxyl Groups on the Structure and Reactivity of Functionalized *m* -Carboranethiolate Self-Assembled Monolayers. *Chem. Mater.* **2020**, *32*, 6800−6809.

(20) Hohman, J. N.; Zhang, P.; Morin, E. I.; Han, P.; Kim, M.; Kurland, A. R.; McClanahan, P. D.; Balema, V. P.; Weiss, P. S. Self-Assembly of Carboranethiol Isomers on Au{111}: Intermolecular Interactions Determined by Molecular Dipole Orientations. *ACS Nano* **2009**, *3*, 527−536.
(21) Kim, J.; Rim, Y. S.; Liu, Y.; Serino, A. C.; Thomas, J. C.; Chen, H.; Yang, Y.; Weiss, P. S. Interface Control in Organic Electronics Using Mixed Monolayers of Carboranethiol Isomers. *Nano Lett.* **2014**, *14*, 2946−2951.
(22) Mete, E.; Yılmaz, A.; Danışman, M. F. A van Der Waals Density Functional Investigation of Carboranethiol Self-Assembled Monolayers on Au(111). *Phys. Chem. Chem. Phys.* **2016**, *18*, 12920−12927.
(23) Yavuz, A.; Sohrabnia, N.; Yilmaz, A.; Danışman, M. F. Mixed Carboranethiol Self-Assembled Monolayers on Gold Surfaces. *Appl. Surf. Sci.* **2017**, *413*, 233−241.
(24) Aoki, T.; Nakahama, Y.; Ikeda, T.; Shindo, M.; Uchiyama, M.; Shudo, K. Electronic States of 3D Aromatic Molecules on Au(111) Surfaces: Adsorption of Carboranethiol. *J. Mater. Sci.* **2019**, *54*, 10249−10260.
(25) Kristiansen, K.; Stock, P.; Baimpos, T.; Raman, S.; Harada, J. K.; Israelachvili, J. N.; Valtiner, M. Influence of Molecular Dipole Orientations on Long-Range Exponential Interaction Forces at Hydrophobic Contacts in Aqueous Solutions. *ACS Nano* **2014**, *8*, 10870−10877.
(26) Yortanlı, M.; Mete, E. Carboxyl- and Amine-Functionalized Carboranethiol SAMs on Au(111): A Dispersion-Corrected Density Functional Theory Study. *Phys. Rev. Mater.* **2020**, *4*, No. 095002.
(27) Kresse, G.; Furthmüller, J. Efficient Iterative Schemes for Ab Initio Total-Energy Calculations Using a Plane-Wave Basis Set. *Phys. Rev. B* **1996**, *54*, 11169−11186.
(28) Kresse, G.; Joubert, D. From Ultrasoft Pseudopotentials to the Projector Augmented-Wave Method. *Phys. Rev. B* **1999**, *59*, 1758−1775.
(29) Blöchl, P. E. Projector Augmented-Wave Method. *Phys. Rev. B* **1994**, *50*, 17953−17979.
(30) Peng, H.; Yang, Z.-H.; Perdew, J. P.; Sun, J. Versatile van Der Waals Density Functional Based on a Meta-Generalized Gradient Approximation. *Phys. Rev. X* **2016**, *6*, No. 041005.
(31) Sun, J.; Ruzsinszky, A.; Perdew, J. P. Strongly Constrained and Appropriately Normed Semilocal Density Functional. *Phys. Rev. Lett.* **2015**, *115*, No. 036402.
(32) Vydrov, O. A.; van Voorhis, T. Nonlocal van Der Waals Density Functional: The Simpler the Better. *J. Chem. Phys.* **2010**, *133*, 244103.
(33) Yortanlı, M.; Mete, E. Common Surface Structures of Graphene and Au(111): The Effect of Rotational Angle on Adsorption and Electronic Properties. *J. Chem. Phys.* **2019**, *151*, 214701.
(34) Ferrighi, L.; Madsen, G. K. H.; Hammer, B. Self-Consistent Meta-Generalized Gradient Approximation Study of Adsorption of Aromatic Molecules on Noble Metal Surfaces. *J. Chem. Phys.* **2011**, *135*, No. 084704.
(35) Shepard, S.; Smeu, M. First Principles Study of Graphene on Metals with the SCAN and SCAN+rVV10 Functionals. *J. Chem. Phys.* **2019**, *150*, 154702.
(36) Patra, A.; Bates, J. E.; Sun, J.; Perdew, J. P. Properties of Real Metallic Surfaces: Effects of Density Functional Semilocality and van Der Waals Nonlocality. *Proc. Natl. Acad. Sci. U. S. A.* **2017**, *114*, No. E9188.
(37) Maksymovych, P.; Sorescu, D. C.; Yates, J. T. Gold-Adatom-Mediated Bonding in Self-Assembled Short-Chain Alkanethiolate Species on the Au(111) Surface. *Phys. Rev. Lett.* **2006**, *97*, No. 146103.
(38) Maksymovych, P.; Voznyy, O.; Dougherty, D. B.; Sorescu, D. C.; Yates, J. T. Gold Adatom as a Key Structural Component in Self-Assembled Monolayers of Organosulfur Molecules on Au(111). *Prog. Surf. Sci.* **2010**, *85*, 206−240.
(39) Colombo, E.; Belletti, G.; Tielens, F.; Quaino, P. Induced Electronic Changes at the Fluorinated Polyphenylthiols on Nanostructured Au(111) Interfaces. *Appl. Surf. Sci.* **2018**, *452*, 141−147.
(40) Pensa, E.; Azofra, L. M.; Albrecht, T.; Salvarezza, R. C.; Carro, P. Shedding Light on the Interfacial Structure of Low-Coverage Alkanethiol Lattices. *J. Phys. Chem. C* **2020**, *124*, 26748−26758.
(41) Smith, R. K.; Reed, S. M.; Lewis, P. A.; Monnell, J. D.; Clegg, R. S.; Kelly, K. F.; Bumm, L. A.; Hutchison, J. E.; Weiss, P. S. Phase Separation within a Binary Self-Assembled Monolayer on Au{111} Driven by an Amide-Containing Alkanethiol. *J. Phys. Chem. B* **2001**, *105*, 1119−1122.
(42) Lewis, P. A.; Smith, R. K.; Kelly, K. F.; Bumm, L. A.; Reed, S. M.; Clegg, R. S.; Gunderson, J. D.; Hutchison, J. E.; Weiss, P. S. The Role of Buried Hydrogen Bonds in Self-Assembled Mixed Composition Thiols on Au{111}. *J. Phys. Chem. B* **2001**, *105*, 10630−10636.
(43) Thomas, J. C.; Goronzy, D. P.; Dragomiretskiy, K.; Zosso, D.; Gilles, J.; Osher, S. J.; Bertozzi, A. L.; Weiss, P. S. Mapping Buried Hydrogen-Bonding Networks. *ACS Nano* **2016**, *10*, 5446−5451.
(44) Ano, T.; Kishimoto, F.; Tsubaki, S.; Lu, Y.-H.; Hohman, J. N.; Maitani, M. M.; Salmeron, M.; Wada, Y. Controlling the Schottky Barrier at the Pt/TiO_2 Interface by Intercalation of a Self-Assembled Monolayer with Oriented Dipole Moments. *J. Phys. Chem. C* **2021**, *125*, 13984−13989.

https://doi.org/10.1021/acsanm.2c02339
ACS Appl. Nano Mater. 2022, 5, 11185−11193